Design of an Unknown Input Observer to Enhance Driver Experience of Electric Power Steering Systems

M. Reichhartinger[1]   S.K. Spurgeon[2]   M. Weyrer[3]

Abstract— **Electric power steering (EPS) systems assist the driver during manoeuvres by applying an additional steering torque generated by an electric motor. Although there are many advantages for electric actuated steering systems including fuel efficiency, they are known to deteriorate the feel of the steering as experienced by the driver. This paper presents a sliding mode observer based estimation concept which provides signals to evaluate and improve perception and feel of the steering as experienced by the driver. The proposed strategy is based on a physically motivated dynamic model of a power steering system and the measurements considered are typically available in any modern vehicle. The performance of the estimator is investigated using numerical simulation as well as experimental results obtained using a laboratory steering testbed.**

I. INTRODUCTION

Power steering systems have a long tradition in automobiles. The basic idea is to assist the driver of an automotive vehicle during steering. The required steering torque introduced by a driver to carry out a desired steering manoeuvre therefore may be significantly reduced. An actuator generating the assistive torque has to be installed in the steering system. The vast majority of power steering systems are actuated by hydraulic actuators. They produce high assistive forces and are characterized by high reliability. The main disadvantage of purely hydraulic driven systems is the energy consumption of the hydraulic pump. Typically it is realized as a constant flow pump connected to the engine via a drive belt. It continuously maintains hydraulic pressure to the steering actuator, even in the case when no assistance is requested. In so-called electrohydraulic systems, an electric motor is used to operate the hydraulic pump. Hence, the hydraulic circuit is decoupled from the engine and the speed of the electric motor can be adjusted according to current steering demands. Although the electrohydraulic system significantly reduces the energy consumption, so-called electric power steering (EPS) systems result [1] whereby the entire hydraulic circuit is replaced by an electric motor and a torque sensor. Besides the motivation to further reduce the power consumption (and therefore improve the fuel economy [2]), the EPS system is introduced as a basis for autonomous driving, active steering and drive by wire applications. In Fig. 1 the two most

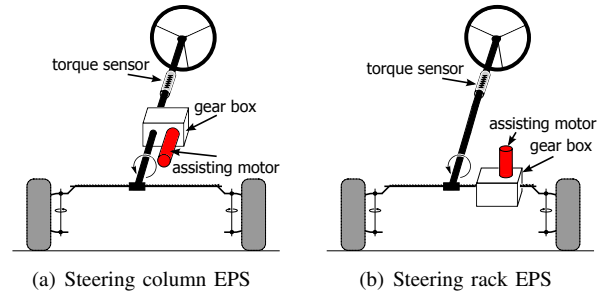

(a) Steering column EPS   (b) Steering rack EPS

Fig. 1: Steering column and steering rack EPS systems

common EPS realizations are shown. The main difference between these two realizations is the place where the assisting torque/force is introduced into the steering system. In the case of a column EPS system, the motor is mounted close to the steering wheel and the assistive torque acts on the steering column as in Fig. 1(a). The steering rack realization (see Fig. 1(b)) is characterized by an assistive force acting on the steering rack. Steering column realizations typically are used in lower and middle value cars. Compared to rack steering realizations, a column steering setup requires less powerful electric motors and consequently less space.
A number of publications concerning the modelling and control of EPS systems are available: A detailed model based on the Bond Graph modelling approach is presented in [3]. The proposed physically motivated model of order 8 is investigated using frequency domain characteristics and step response experiments. In [2] an overview of different EPS realizations and different types of electric drives used in the context of EPS are discussed. The motor of an EPS system may also be used for enhanced parking assistance, steering speed dependent assistance and lane keeping or active return applications [4], [5]. A frequently implemented control approach is a map based actuation of the motor. These so-called boost curves use the steering force/torque introduced by the driver and the vehicle speed to determine the assistance torque [6]. Advanced control methods e.g. based on optimization and H_∞ controller design techniques, are applied in [7], [8], [9]. A loopshaping method and a hydraulic actuated setup including boost curve actuation for an automated highway system is considered in [10]. A combined Fuzzy - PID control concept is proposed in [11]. Although the fuzzy rules are explained in detail, the reference torque of the controller is also assumed to be available for map based evaluation of the applied steering torque. The control approach is investigated using a step response

[1]Markus Reichhartinger is with the Faculty of Electrical and Information Engineering, Institute of Automation and Control, Graz University of Technology, 8010 Graz, Austria markus.reichhartinger@tugraz.at

[2]Sarah K. Spurgeon is with the School of Engineering and Digital Arts, University of Kent, Canterbury, Kent CT2 7NT, UK S.K.Spurgeon@kent.ac.uk

[3]M. Weyrer is with the Faculty of Technical Sciences, Institute of Networked and Embedded Systems at Alpen-Adria Universität Klagenfurt, 9020 Klagenfurt, Austria matthias.weyrer@aau.at

simulation scenario. Ideas on fuzzy control techniques also are used in [12], where the return-to-centre problem of EPS systems is covered. This problem is frequently present in EPS systems and originates from the installed motor which increases the moment of inertia and introduces additional friction into the system. As a consequence, the steering wheel does not return to the centre when the driver does not apply any steering torque when the car is moving.

It is known from test track experiments and also from assessment tests[1] that EPS systems already provide satisfying performance against many evaluation criteria. However, the driver perception of road and steering feedback (see e.g. [13]) remains problematic. An important quantity relating to the current force and torque at the tyres is the, typically unmeasured, rack force. This paper estimates this force using a sliding-mode observer. Such an estimate can inform an EPS control scheme which considers the rack force in order to improve the road feedback experienced by the driver. A different mathematical model to that given in [14], [15] is proposed. Additionally the implementation of differentiators suggested in [16], [17] is avoided. It is demonstrated that although the so-called observer matching conditions are not satisfied the implementation of differentiators as frequently suggested in the literature is not required.

The paper is organized as follows: In section II the mathematical model of the EPS system is presented and the problem formulation is given. The observer based estimator is designed in section III. Results obtained by numerical simulations and real world experiments are shown in sections IV and V.

II. PROBLEM FORMULATION

In Fig. 2 a schematic diagram of the considered column EPS setup is depicted. At the steering wheel, the steering torque T_d is applied by the driver. The angular velocity and the angle of the steering wheel are denoted by ω_s and φ_s respectively. The torque sensor divides the steering column into two parts. The upper part consists of the steering wheel and the steering column. The lower part consists of the steering rack, the dc motor, gear box, the intermediate shaft and the steering pinion. The latter is used to transform the rotational movement of the intermediate shaft into translational movement of the steering rack. Gear backlash introduced by the pinion and the gear box are neglected. The differential equations governing the movement of the steering system are

$$I_s \frac{d\omega_s}{dt} = T_d - k_s (\varphi_s - \varphi_t) - d_s\omega_s, \tag{1a}$$

$$I_t \frac{d\omega_t}{dt} = k_s (\varphi_s - \varphi_t) + r_m T_m - d_m\omega_t - r_t F, \tag{1b}$$

where ω_t and φ_t denote the angular velocity and the position of the intermediate shaft respectively. Both the movement of the steering column and the intermediate shaft are affected by
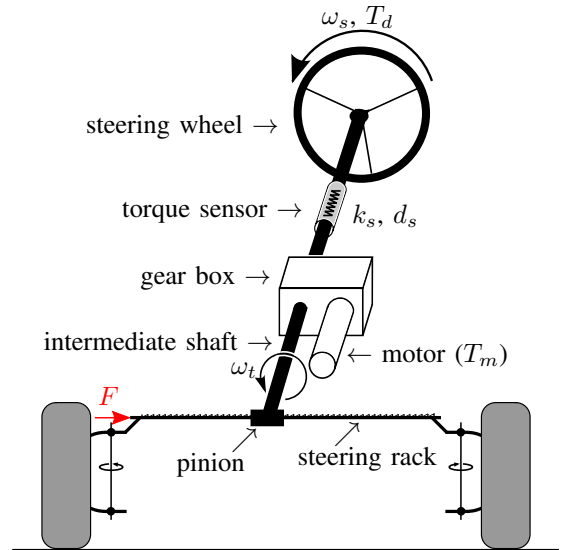
Fig. 2: Schematic diagram of the considered EPS setup.

viscous friction with coefficients d_m and d_s. The stiffness of the torque sensor is given by k_s. The gear ratio of the gear box is given by r_m and the pinion radius is given by r_t. The torque introduced by the electric motor is given by T_m. The moment of inertia of the steering wheel and the steering column is represented by I_s. The moment of inertia I_t is determined by the mass m of the steering rack, the moment of inertia I_m of the motor and the moment of inertia of the intermediate shaft I_c, i.e.

$$I_t = I_c + r_m^2 I_m + r_t^2 m. \tag{2}$$

Using the definition of the state variables $x_1 := \omega_s$, $x_2 := \omega_t$ and $x_3 := \varphi_s - \varphi_t$ the differential equations (1) become

$$\frac{d\mathbf{x}}{dt} = \mathbf{A}\mathbf{x} + \mathbf{b}T_m + \mathbf{D}\mathbf{w} \tag{3a}$$

$$\mathbf{y} = \mathbf{C}\mathbf{x} \tag{3b}$$

where

$$\mathbf{A} := \begin{bmatrix} -\frac{d_s}{I_s} & 0 & -\frac{k_s}{I_s} \\ 0 & -\frac{d_m}{I_t} & \frac{k_s}{I_t} \\ 1 & -1 & 0 \end{bmatrix}, \mathbf{b} := \begin{bmatrix} 0 \\ \frac{r_m}{I_t} \\ 0 \end{bmatrix},$$

$$\mathbf{D} := \begin{bmatrix} \frac{1}{I_s} & 0 \\ 0 & -\frac{r_t}{I_t} \\ 0 & 0 \end{bmatrix}, \mathbf{w} = \begin{bmatrix} T_d \\ F \end{bmatrix}, \mathbf{C} = \begin{bmatrix} 1 & 0 & 0 \\ 0 & 0 & k_s \end{bmatrix}. \tag{4}$$

The output $\mathbf{y}$ represents the measured variables

$$y_1 := x_1, \quad \text{and} \quad y_2 := k_s x_3, \tag{5}$$

where y_1 represents the angular velocity of the steering wheel and y_2 is the signal measured by the torque sensor. These measurements are typically available in any conventional EPS system. The input vector $\mathbf{w}$ comprises the unknown inputs, the driver torque T_d and the rack force F. The objective is to provide estimates of the unknown input $\mathbf{w}$ and the unknown state variable x_2. These signals are required by enhanced EPS control architectures which provide power assisted steering combined with satisfactory road-to-driver feedback.

III. AN UNKNOWN INPUT OBSERVER

An observer to estimate the unknown state variable x_2 and the unknown input $\mathbf{w}$ is designed[2]. Note that the structure of system (3) exactly corresponds with systems discussed in [18], [19], [20]. In order to follow these approaches, the invariant zeros of $\{\mathbf{A}, \mathbf{D}, \mathbf{C}\}$ have to be located in $\mathbb{C}_-$ and the observer matching condition

$$\text{rank}(\mathbf{CD}) \overset{!}{=} \text{rank}(\mathbf{D}) \overset{!}{=} m, \tag{6}$$

where m denotes the number of unknown inputs must be satisfied. The system (3) has no invariant zeros but the observer matching condition is violated as $\text{rank}(\mathbf{D}) = 2$ and $\text{rank}(\mathbf{CD}) = 1$. A remedy for this situation is presented in [21, Part IV] where the presented algorithm first transforms the system into a so-called quasi block triangular observable form and successive application of super-twisting differentiators yields the desired finite estimation error convergence. With this approach it is not guaranteed apriori that the proposed transformation yields the desired representation for observer design. Another approach available in the literature is to consider an augmented output composed of the measured outputs and their derivatives as a new output [22]. This technique is used in [17] and two additional differentiators are implemented in order to satisfy the observer matching condition. In this paper additional differentiators are avoided by exploiting the system structure. The unknown input T_d is reconstructed independently of the estimation of x_2 and F. Therefore, the design of the observer consists of two parts: The estimations of T_d, see section III-A and the estimation of x_2 and F, see section III-B

A. Estimation of T_d

From (3), consider the differential equation describing y_1:

$$\frac{dy_1}{dt} = -\frac{d_s}{I_s} y_1 - \frac{1}{I_s} y_2 + \frac{1}{I_s} T_d \tag{7}$$

The observer is given by

$$\frac{d\hat{y}_1}{dt} = -\frac{d_s}{I_s} y_1 - \frac{1}{I_s} y_2 + \kappa_1 \lfloor y_1 - \hat{y}_1 \rceil^{1/2} + w_1, \tag{8a}$$

$$\frac{dw_1}{dt} = \kappa_2 \lfloor y_1 - \hat{y}_1 \rceil^0, \tag{8b}$$

where $\lfloor y_1 - \hat{y}_1 \rceil^k := |y_1 - \hat{y}_1|^k \, \text{sign}\,(y_1 - \hat{y}_1)$. The dynamics of the estimation error $e_1 := y_1 - \hat{y}_1$ is governed by

$$\frac{de_1}{dt} = \frac{1}{I_s} T_d - \kappa_1 \lfloor e_1 \rceil^{1/2} - w_1, \tag{9}$$

As $z_1 := \frac{1}{I_s} T_d - w_1$, the error dynamics may be written as

$$\frac{de_1}{dt} = z_1 - \kappa_1 \lfloor e_1 \rceil^{1/2}, \tag{10a}$$

$$\frac{dz_1}{dt} = \frac{1}{I_s} \frac{dT_d}{dt} - \kappa_2 \lfloor e_1 \rceil^0. \tag{10b}$$

[2]Note that the variable x_1 is available from measurement and x_3 may be computed using y_2, see equation (5).

Assume the steering torque applied by the driver satisfies

$$\left| \frac{dT_d}{dt} \right| \leq L_1. \tag{11}$$

Choosing the constant observer parameters according to

$$\kappa_1 = 1.5 \sqrt{\frac{L_1}{I_s}} \quad \text{and} \quad \kappa_2 = 1.1 \frac{L_1}{I_s} \tag{12}$$

ensures that e_1 and z_1 converge to zero within finite time (see e.g. [23], [24]) and the applied driver torque T_d may be reconstructed as $\hat{T}_d := I_s w_1$.

B. Estimation of x_2 and reconstruction of F

The observer design to estimate x_2 follows the same procedure as applied in section III-A. Here, the dynamic behaviour of the output y_2, the measured torque, is exploited. From equation (3)

$$\frac{dy_2}{dt} = k_s y_1 - k_s x_2. \tag{13}$$

The following observer is proposed

$$\frac{d\hat{y}_2}{dt} = k_s y_1 + \kappa_3 \lfloor y_2 - \hat{y}_2 \rceil^{1/2} + w_2, \tag{14a}$$

$$\frac{dw_2}{dt} = \kappa_4 \lfloor y_2 - \hat{y}_2 \rceil^0. \tag{14b}$$

The estimation error dynamics is given by

$$\frac{de_2}{dt} = z_2 - \kappa_3 \lfloor e_2 \rceil^{1/2}, \tag{15a}$$

$$\frac{dz_2}{dt} = -k_s \frac{dx_2}{dt} - \kappa_4 \lfloor e_2 \rceil^0, \tag{15b}$$

where $e_2 := y_2 - \hat{y}_2$ and $z_2 := -k_s x_2 + w_2$. Assuming that the angular acceleration of the intermediate shaft is bounded by

$$\left| \frac{dx_2}{dt} \right| \leq L_2 \tag{16}$$

the constant observer parameters are selected as

$$\kappa_3 = 1.5 \sqrt{k_s L_2} \quad \text{and} \quad \kappa_4 = 1.1 k_s L_2. \tag{17}$$

This choice ensures that the trajectories of system (15) converge to zero and the angular velocity of the intermediate shaft is reconstructed by

$$\hat{x}_2 := \frac{w_2}{k_s}. \tag{18}$$

The estimate of the rack force F is based on the observer

$$\frac{dz_3}{dt} = -\frac{d_m}{I_t} \hat{x}_2 + \frac{1}{I_t} y_2 + \frac{r_m}{I_t} T_m + \nu_3 (\hat{x}_2 - z_3) \tag{19}$$

which relies on the estimate given in (18). The injection term ν_3 is designed as

$$\nu_3 (\hat{x}_2 - z_3) = \kappa_5 \lfloor \hat{x}_2 - z_3 \rceil^{1/2} - w_3, \tag{20a}$$

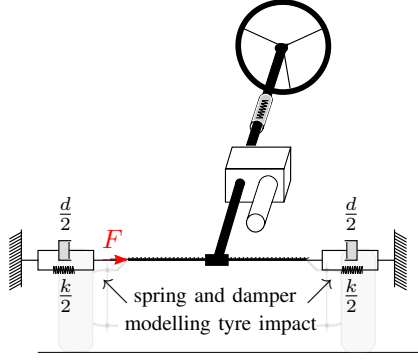$$\frac{dw_3}{dt} = \kappa_6 \lfloor \hat{x}_2 - z_3 \rceil^0. \tag{20b}$$

Fig. 3: The impact of the tyres is modeled by a spring and damper setup.

Introducing the error $e_3 := \hat{x}_2 - z_3$ and assuming $x_2 = \hat{x}_2$, the estimation error dynamics is

$$\frac{de_3}{dt} = \frac{d}{dt}(x_2 - z_3) \overset{x_2 \equiv \hat{x}_2}{=} -\frac{r_t}{I_t}F - \nu_3(e_3). \tag{21}$$

It is assumed that the time derivative of the rack force F is a Lipschitz function, i.e.

$$\left|\frac{dF}{dt}\right| \leq L_3, \tag{22}$$

with an unknown Lipschitz constant L_3. In contrast to the previous designed constant gain observers, the Lipschitz constant L_3 is difficult to estimate. Therefore, an adaptive gain observer given by

$$\frac{d\kappa_5}{dt} = \begin{cases} \alpha \, \text{sign}(|e_3| - \beta) & \text{for } \kappa_5 > \delta \\ \gamma & \text{for } \kappa_5 \leq \delta \end{cases} \tag{23a}$$

$$\kappa_6 = \varepsilon \kappa_5 \tag{23b}$$

is implemented [25]. Here α, β, γ, δ and ε denote positive constants. The gains κ_5 and κ_6 vary with time such that the error signal e_3 converges into a narrow domain specified by β. As long as e_3 belongs to this domain, the gains are reduced until either e_3 leaves the domain or the observer gain κ_5 reaches its lower limit given by δ. The adaptation parameter α defines the rate of change of the observer parameters. The trajectories of system (21) therefore converge to $|e_3| \leq \beta$ and remain there. Assuming that β is selected sufficiently small, i.e $\beta \approx 0$, the rack force F may be estimated by

$$\hat{F} = \frac{I_t}{r_t} w_3. \tag{24}$$

IV. NUMERICAL SIMULATION

The system given in equations (3), (4) and (5) is implemented in Matlab/Simulink. In order to generate the unknown rack force, the setup depicted in Fig. 3 is considered and the impact of the tyres is modelled by a spring and damper setup producing a force according to

$$F = d \, r_t \, \omega_t + k \, r_t \, \varphi_t, \tag{25}$$

where d and k denote the damping and spring coefficients respectively. The system parameters used are listed in Table

I. The constant observer parameters κ_1, κ_2, κ_3 and κ_4 are chosen based on measured signals from the testbed described in section V. It is known that in general the absolute value of the applied steering torque does not exceed $5Nm$. Under harsh conditions, it is assumed that a driver changes the steering direction abruptly and 0.2 seconds are required to reapply the maximum steering torque (e.g. from $5Nm$ to $-5Nm$). This yields $L_1 = 50$ and κ_1 and κ_2 are selected as given in equation (12). The constant L_2, see equation (16), is obtained via numerical differentiation of available measurements. This reveals that $L_2 = 100 \, rad/s^2$, which is used to determine κ_3 and κ_4, see equation (17). The parameters of the adaptation law (23) are selected following several simulation scenarios and are chosen as $\alpha = 800$, $\beta = 0.1$, $\gamma = 1$, $\delta = 18$ and $\varepsilon = 21$. The assistive torque T_m applied by the motor is computed by a boost curve as suggested in [7]. In order to excite the system by an appropriate steering action, a steering controller was implemented. It applies a steering torque T_d such that the steering angle φ_s tracks a given reference. Here, the steering angle depicted in Fig. 4 and a fixed step solver with $1ms$ step size were used. The applied steering angle consists of 3 parts: For the first 11 seconds, the signal is captured by a real world experiment. The steering controller tracks a constant reference signal in the second phase which ends at 14 seconds. The third phase immediately returns the desired steering wheel to the zero position and starts with a zig-zag steering manoeuvre of increasing frequency until the simulation ends. In order to demonstrate the impact of the unknown force F computed by equation (25), the parameter k was changed during the simulation experiment. For the first 11 seconds it is kept constant before being gradually increased. This behaviour becomes evident in Fig. 5 (during the time interval from 11 to 14 seconds). The absolute values of the depicted torques have to be increased in order to keep the steering angle at a constant value. In Fig. 6 the estimation errors with respect to x_2 and T_d are plotted. Fig. 7 shows the evolution of the rack force estimate as well as the behaviour of the adaptive gain κ_5.

TABLE I: Parameters of the EPS testbed

| Description	Symbol	Value	Unit
inertia steering wheel and steering column	I_s	0.02329	$kg \cdot m^2$
moment of inertia of intermediate shaft	I_c	0.008	$kg \cdot m^2$
moment of inertia of motor shaft	I_m	0.0004	$kg \cdot m^2$
mass of the steering rack	m	4.7	kg
damping coefficient: steering column	d_s	0.26645	$Nm\,s/rad$
damping coefficient: intermediate shaft and motor	d_m	0.0028	$Nm\,s/rad$
spring constant of the torque sensor	k_s	142.58	Nm/rad
pinion radius	r_t	0.0115	m
gear ratio: motor - intermediate shaft	r_m	18	-
damping coefficient: tyre model	d	5000	Ns/m
spring constant: tyre model	k	54000	N/m
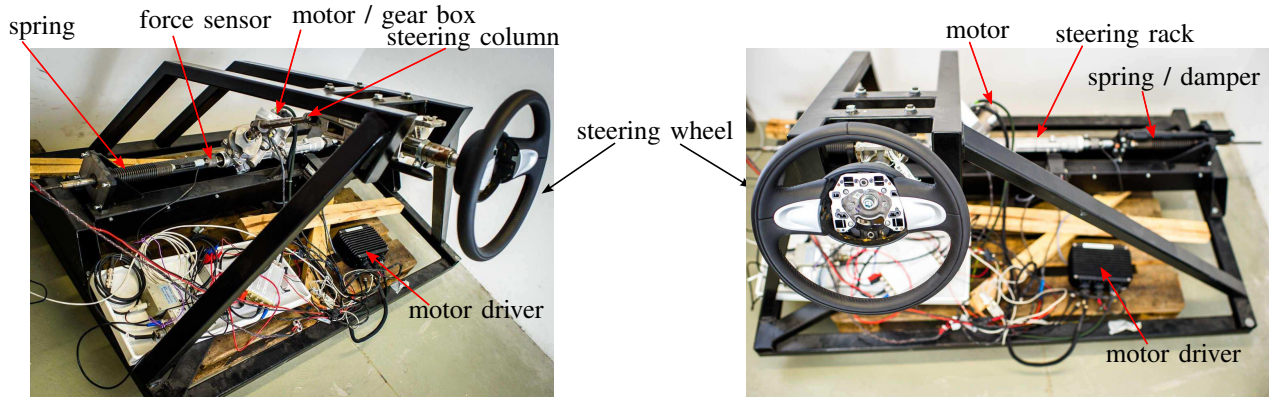
Fig. 8: Experimental EPS testbed.
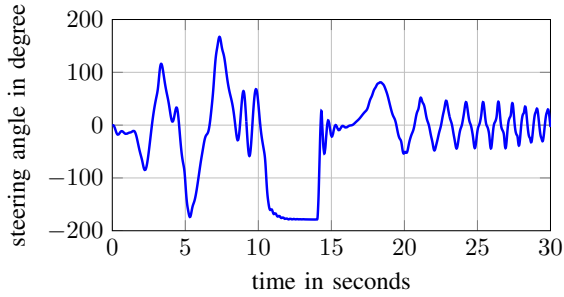
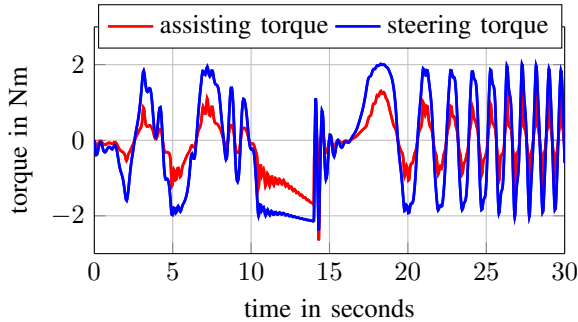Fig. 4: Steering angle used for numerical simulation.

Fig. 6: Estimation error signals during simulation.

Fig. 5: Steering torque T_d and assisting torque T_m applied by the electric motor.

Fig. 7: Evolution of the rack force F, its estimated value $\hat{F}$ (labeled as estimated force) and the behavior of the adaptive gain κ_5.

V. EXPERIMENTAL RESULTS

Real world experiments were conducted using the test-bench depicted in Fig. 8. It consists of an EPS system formerly installed on a Mini Cooper. In addition to the pre-installed sensors (e.g a steering column torque sensor), force sensors in the steering rack, a steering rack position sensor, an advanced steering angle and steering angular velocity sensor are installed. A dSpace Microautobox serves as the control unit. It communicates with the motor control unit via a CAN bus. The motor current, the motor position and the motor angular velocity are measured by the motor control unit. A sensor to measure the steering torque T_d is not installed. However, in order to validate the estimated values of the observer designed in section IV, T_d was computed using equation (1a) and equation (5). The experimental results are obtained using a sampling period of $1ms$. During
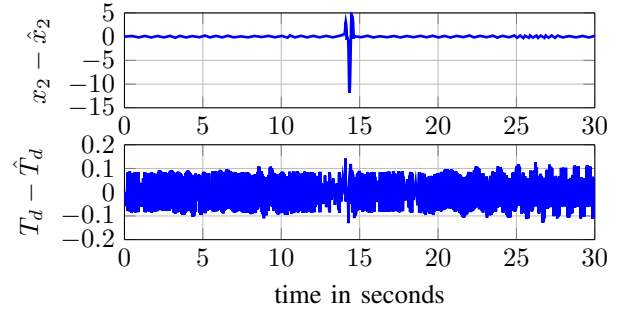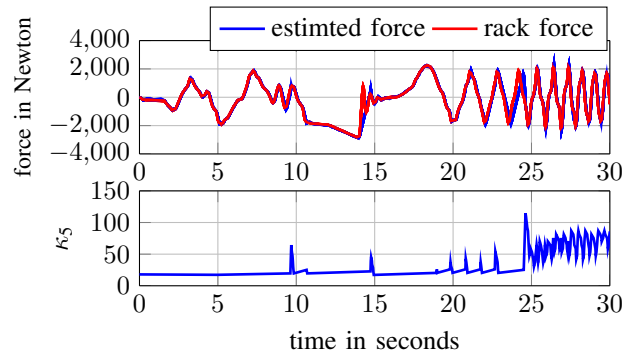
the experiments, an EPS control strategy including an active return functionality was activated. Hence, the driver was assisted during steering. The setting of the constant observer parameters κ_1, κ_2, κ_3 and κ_4 as explained in section IV was also used for the experiments. The adaptation gains were selected as $\delta = 680$ and $\varepsilon = 2$. The remaining gains are selected as in the simulations. Fig. 9 shows the steering angle applied at the EPS testbench during the experiment. The estimated values are plotted in Fig. 10.

VI. CONCLUSION

EPS systems are known to reduce energy consumption in automobiles and also provide a basis for automotive applications such as active steering and lane keeping assistance. The
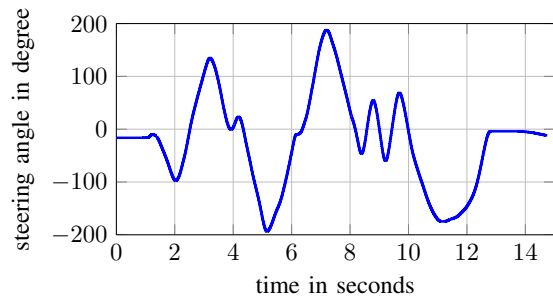
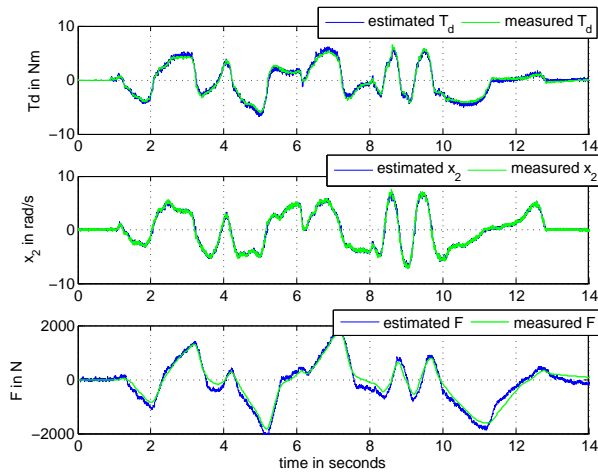Fig. 9: Evolution of the steering angle during the experiments

Fig. 10: Experimental results obtained by the proposed scheme.

construction of EPS systems is simple and minimises space and component requirements. The assistive torque produced by the motor of an EPS system is computed by an EPS control concept. The major drawback of EPS systems is reduced road-to-driver-feedback. In this paper a sliding-mode observer is proposed to estimate signals which are required by EPS control strategies to improve integrated road-to-driver feedback. The observer uses signals which are measured in any modern vehicle. The performance is demonstrated using numerical simulation and real world experiments.

ACKNOWLEDGEMENT

REFERENCES

[1] A. DellAmico and P. Krus, "Modeling, simulation, and experimental investigation of an electrohydraulic closed-center power steering system," *IEEE/ASME Transactions on Mechatronics,*, pp. 1–11, 2015.

[2] A. Burton, "Innovation drivers for electric power-assisted steering," *IEEE Control Systems*, vol. 23, no. 6, pp. 30–39, Dec 2003.

[3] L. an Wang, Q. Li, and X. juan Liang, "Modeling and dynamic simulation of electric power steering system of automobile using bond graph technique," in *Third International Symposium on Intelligent Information Technology and Security Informatics (IITSI)*, April 2010, pp. 744–747.

[4] S. Yang, X. Guo, B. Yang, and G. Tan, "Return-to-center control of electric power steering," in *9th International Conference on Electronic Measurement Instruments, 2009. ICEMI '09.*, Aug 2009.

[5] M. Bröcker, "New control algorithms for steering feel improvements of an electric powered steering system with belt drive," *Vehicle System Dynamics*, vol. 44, no. sup1, pp. 759–769, 2006.

[6] J.-H. Kim and J.-B. Song, "Control logic for an electric power steering system using assist motor," *Mechatronics*, vol. 12, no. 3, pp. 447 – 459, 2002.

[7] R. C. Chabaan and L. Y. Wang, "Control of electrical power assist systems: Hinfty design, torque estimation and structural stability," *JSAE Review*, vol. 22, no. 4, pp. 435 – 444, 2001.

[8] F. Zhao, K. Guo, J. Zhang, L. Zhang, F. Li, and L. Yang, "A study on h infinity control in electric power steering system," in *International Conference on Electronic and Mechanical Engineering and Information Technology (EMEIT),*, vol. 7, Aug 2011, pp. 3599–3602.

[9] A. Zaremba, M. Liubakka, and R. Stuntz, "Control and steering feel issues in the design of an electric power steering system," in *Proceedings of the 1998 American Control Conference,*, vol. 1, Jun 1998, pp. 36–40 vol.1.

[10] P. Hingwe, M. Tai, and M. Tomizuka, "Modeling and robust control of power steering system of heavy vehicles for ahs," in *Proceedings of the 1999 IEEE International Conference on Control Applications, 1999.*, vol. 2, 1999, pp. 1365–1370 vol. 2.

[11] Z. Gao, W. Wu, J. Zheng, and Z. Sun, "Electric power steering system based on fuzzy pid control," in *9th International Conference on Electronic Measurement Instruments, 2009. ICEMI '09.*, Aug 2009, pp. 3–456–3–459.

[12] Z. Yan and L. Fei, "Research on dynamic behavior of eps based on frequency response and step response," in *5th International Conference on Computer Science and Education (ICCSE),*, Aug 2010, pp. 1332–1335.

[13] D. Katzourakis, J. C. de Winter, S. de Groot, and R. Happee, "Driving simulator parameterization using double-lane change steering metrics as recorded on five modern cars," *Simulation Modelling Practice and Theory*, vol. 26, pp. 96 – 112, 2012.

[14] A. Marouf, M. Djemai, C. Sentouh, and P. Pudlo, "A new control strategy of an electric-power-assisted steering system," *IEEE Transactions on Vehicular Technology*, vol. 61, no. 8, pp. 3574–3589, Oct 2012.

[15] A. Marouf, C. Sentouh, M. Djemai, and P. Pudlo, "Control of an electric power assisted steering system using reference model," in *50th IEEE Conference on Decision and Control and European Control Conference (CDC-ECC)*, Dec 2011, pp. 6684–6690.

[16] L. Nehaoua, M. Djemai, and P. Pudlo, "Rack force feedback for an electrical power steering simulator," in *20th Mediterranean Conference on Control Automation (MED),*, July 2012, pp. 79–84.

[17] A. Marouf, M. Djemai, C. Sentouh, and P. Pudlo, "Driver torque and road reaction force estimation of an electric power assisted steering using sliding mode observer with unknown inputs," in *13th International IEEE Conference on Intelligent Transportation Systems (ITSC)*, Sept 2010, pp. 354–359.

[18] T. Floquet, C. Edwards, and S. K. Spurgeon, "On sliding mode observers for systems with unknown inputs," *International Journal of Adaptive Control and Signal Processing*, vol. 21, no. 8-9, pp. 638–656, 2007.

[19] W. Perruquetti and J. P. Barbot, *Sliding Mode Control in Engineering*. Marcel Dekker AG, Switzerland, 2002.

[20] S. Hui and S. Zak, "Observer design for systems with unknown inputs," *International Journal of Applied Mathematics and Computer Science*, vol. 15, no. 4, pp. 431–446, 2005.

[21] C. Edwards, E. Fossas Colet, and L. Fridman, Eds., *Advances in Variable Structure and Sliding Mode Control*, ser. Lecture Notes in Control and Information Sciences, 334. Springer-Verlag Berlin Heidelberg, 2006.

[22] M. T. Angulo, J. A. Moreno, and L. Fridman, "On functional observers for linear systems with unknown inputs and hosm differentiators," *Journal of the Franklin Institute*, vol. 351, no. 4, pp. 1982 – 1994, 2014.

[23] Y. Shtessel, C. Edwards, L. Fridman, and A. Levant, *Sliding Mode Control and Observation*. Birkhäuser, Springer Science+Business Media, New York, 2014.

[24] A. Levant, "Homogeneity approach to high-order sliding mode design," *Automatica*, vol. 41, no. 5, pp. 823 – 830, 2005.

[25] Y. Shtessel, M. Taleb, and F. Plestan, "A novel adaptive-gain supertwisting sliding mode controller: Methodology and application," *Automatica*, vol. 48, no. 5, pp. 759 – 769, 2012.